Published in final edited form as:
J Biomol NMR. 2008 November ; 42(3): 197–207. doi:10.1007/s10858-008-9272-0.

Solution structure of the Grb2 SH2 domain complexed with a high-affinity inhibitor

Kenji Ogura
Department of Structural Biology, Graduate School of Pharmaceutical Sciences, Hokkaido University, N12 W6, Kita-ku, Sapporo 060-0812, Japan

Takanori Shiga
Department of Structural Biology, Graduate School of Pharmaceutical Sciences, Hokkaido University, N12 W6, Kita-ku, Sapporo 060-0812, Japan

Masashi Yokochi
Department of Structural Biology, Graduate School of Pharmaceutical Sciences, Hokkaido University, N12 W6, Kita-ku, Sapporo 060-0812, Japan

Satoru Yuzawa
Department of Structural Biology, Graduate School of Pharmaceutical Sciences, Hokkaido University, N12 W6, Kita-ku, Sapporo 060-0812, Japan

Terrence R. Burke Jr.
National Cancer Institute at Frederick, Laboratory of Medicinal Chemistry, Center for Cancer Research, P. O. Box B, Frederick, MD 21702-1201, USA

Fuyuhiko Inagaki
Department of Structural Biology, Graduate School of Pharmaceutical Sciences, Hokkaido University, N12 W6, Kita-ku, Sapporo 060-0812, Japan finagaki@pharm.hokudai.ac.jp

Abstract

The solution structure of the growth factor receptor-bound protein 2 (Grb2) SH2 domain complexed with a high-affinity inhibitor containing a non-phosphorus phosphate mimetic within a macrocyclic platform was determined by nuclear magnetic resonance (NMR) spectroscopy. Unambiguous assignments of the bound inhibitor and intermolecular NOEs between the Grb2 SH2 domain and the inhibitor was accomplished using perdeuterated Grb2 SH2 protein. The well-defined solution structure of the complex was obtained and compared to those by X-ray crystallography. Since the crystal structure of the Grb2 SH2 domain formed a domain-swapped dimer and several inhibitors were bound to a hinge region, there were appreciable differences between the solution and crystal structures. Based on the binding interactions between the inhibitor and the Grb2 SH2 domain in solution, we proposed a design of second-generation inhibitors that could be expected to have higher affinity.

Correspondence to: Fuyuhiko Inagaki.

PDB and Bmrb accession code
The atomic coordinates, distance restraints and resonance assignments were deposited in the RCSB Protein Data Bank and the Biological Magnetic Resonance Data Bank with the accession code 1X0N and 11055, respectively.

Supplementary material
Supplementary material is available in electric format and describes the resonance assignment of the inhibitor bound to Grb2 SH2 and residue library file of the inhibitor for the Cyana.

Keywords

Perdeuterated Grb2 SH2; Solution structure; Inhibitor; Structure-based drug design

Introduction

Growth factor receptor-bound protein 2 (Grb2) (Lowenstein et al. 1992) is an adaptor protein having an SH3-SH2-SH3 domain structure. The two SH3 domains of Grb2 bind to proline-rich sequences in the carboxyl terminal region of the nucleotide exchange factor, Sos, in the cytosol (Li et al. 1993; Buday and Downward 1993; Gale et al. 1993). After EGF stimulation, the Grb2 SH2 domain binds to the EGF receptor directly or indirectly through proteins such as Shc, FAK, Syp, and IRS-1, by recognizing phosphotyrosine (pTyr)-containing sequences. It then relocates Sos close to the plasma membrane where interaction with Ras can occur (Rozakis-Adcock et al. 1992; Skolnik et al. 1993a, b; Pronk et al. 1994; Schlaepfer et al. 1994). Thus, Grb2 mediates signal transduction from a variety of extracellular stimuli to Ras. Overexpression of Grb2 has been correlated with liver tumorigenesis in mice and the proliferation of human breast cancer cells (Daly et al. 1994; Yip et al. 2000). Therefore, the development of Grb2 SH2 domain-binding inhibitors could be an effective approach to block the growth of malignant cells.

SH2 domains constitute a characteristic family of protein–protein interaction modules that mediate the formation of multi-protein complexes during cell signaling (Marengere and Pawson 1994). SH2 domains recognize pTyr residues in combination with several additional residues C-terminal to the pTyr. Consensus pTyr-containing sequences binding to the Grb2 SH2 domain have been extensively studied by site-directed mutagenesis, phosphopeptide inhibition, and peptide library screening (Songyang et al. 1994), and the recognition motif is accepted as pTyr-(Leu/Val)-Asn-(Val/Pro). The Asn residue at the pTyr+2 position is essential, implying that Grb2 SH2 domains recognize pTyr-containing sequences in a sequence-specific manner. The recognition modes of pTyr-containing peptides by SH2 domains have been extensively studied by X-ray crystallography and NMR spectroscopy (Kuriyan and Cowburn 1997) and most SH2 domains bind their peptide ligands in an extended conformation. In contrast, the Grb2 SH2 domain binds high affinity ligands in β-turn conformations (Rahuel et al. 1996; Ogura et al. 1999). This unique binding mode suggests that highly specific inhibitors could be developed for this domain (Burke 2006).

A pTyr-containing tripeptide, Ac-pTyr-Ile-Asn-NH_2, originally reported by Novartis Corp. with micromolar affinity to the Grb2 SH2 domain, was a starting point for the improvement of binding affinity (Furet et al. 1997). First, the (pTyr+1) Ile was replaced by an aminocyclohexane carboxylic acid (Ac_6c), which adopted a right-handed 3_{10} helical backbone conformation that stabilized the type-I β-turn and maintained multiple hydrophobic contacts with the surface of the Grb2 SH2 domain (Garcia-Echeverria et al. 1998). The crystal structure of the Grb2 SH2-tripeptide complex also indicated that the C-terminal portion of bound Ac-pTyr-Ile-Asn-NH_2 forms van der Waals contacts with hydrophobic patches on the surface of the SH2 domain (Furet et al. 1999). Thus, the addition of 3-naphthalene-1-yl-propyl functionality at the C-terminus improved the binding affinity by 25-fold (Furet et al. 1998). As the protein tyrosine phosphatase activity is constitutively high in the cytosol, the stability of the phosphate linkage is a major concern in vivo. Substitution of pTyr with phosphonomethyl phenylalanine (Pmp) led to protection from phosphatase-mediated hydrolysis with little loss of binding affinity (Domchek et al. 1992). Finally, in order to stabilize a β-turn conformation, the linear peptide backbone was constrained by macrocyclization (Gao et al. 2001a, b). The resulting cyclic analogue exhibited approximately 100-fold higher binding affinity in vitro relative to its linear

counterpart (Gao et al. 2001a). Therefore, we decided to solve the structure of the macrocyclic inhibitor bound to the Grb2 SH2 domain in order to gain insights into the physical basis of this high affinity binding.

Recently, Phan and co-workers reported the X-ray crystal structure of a high-affinity inhibitor complexed with the Grb2 SH2 domain (Phan et al. 2005; PDB ID 2AOB). Although the inhibitor used in the X-ray crystallography was subtly different at the periphery than the NMR inhibitor; the phosphonomethyl group was replaced with a malonyl group and a α-CH_2CO_2H moiety was added in the pTyr-mimicking portion. Interestingly, two SH2 domains exchanged helices with each other to form a domain-swapped dimer. Moreover, inhibitors were bound to additional sites around the hinge as well as within the canonical pTyr binding site of the SH2 domain. Since these structural features might be induced by crystallization effects, we undertook a solution structural study of the Grb2 SH2 domain bound to the high-affinity inhibitor by NMR spectroscopy.

Materials and methods

Protein expression and purification

The Grb2 SH2 domain (residues 58–159) was expressed and purified as described previously (Tsuchiya et al. 1999). Briefly, the Grb2 SH2 domain cloned into a pGEX-4T-2 vector (GE Healthcare Bio-Sciences) was expressed as a GST fusion protein in *Escherichia coli* BL21(DE3). For preparation of the $^{13}C/^{15}N$ labeled protein, transformed cells were grown in M9 minimal medium containing $^{15}NH_4Cl$ (1 g/l), Celtone-CN (Spectra Stable Isotopes) (1 g/l) and $^{13}C_6$-glucose (4 g/l). The GST fusion protein was purified using Glutathione Sepharose 4B beads (GE Healthcare Bio-Sciences) and was cleaved with trypsin. The Grb2 SH2 domain was further purified using a Resource S column (GE Healthcare Bio-Sciences) and a Superdex 75 column (GE Healthcare Bio-Sciences). To prepare the $^{2}H/^{15}N$-labeled Grb2 SH2 domain, cells were grown in a medium containing 99% $^{2}H_2O$, Celtone-DN (Spectra Stable Isotopes), and ^{2}H-glucose. The protein was concentrated by a Centriprep YM-3 (Amicon) to a final concentration of 0.5 mM.

Analytical size exclusion chromatography

Size exclusion chromatography was carried out at 25°C using a Superdex 75 10/300 GL column attached to an ÄKTA Purifier (GE Healthcare Bio-Sciences). Sample solution containing 0.1 mM of purified Grb2 SH2 domain and 0.9 mM of the macrocyclic inhibitor was passed over the Superdex column equilibrated with phosphate-buffered salines (pH 7.4). The sample solution (0.1 ml) was eluted at flow rate of 0.8 ml/min, and the fractions were monitored by absorbance at 280 nm. The column was calibrated using the following molecular mass standards: bovine serum albumin (67 kDa), ovalbumin (43 kDa), chymotrypsinogen (25 kDa), and RNase A (13.7 kDa) (GE Healthcare Bio-Sciences). A standard curve for molecular mass was constructed by plotting molecular mass against retention volume.

NMR spectroscopy

The macrocyclic inhibitor, prepared as described previously (Gao et al. 2001b), was dissolved in 20 mM sodium phosphate buffer (pH 6.3) to a final concentration of 10 mM. NMR samples contained 0.5 mM Grb2 SH2 domain, with the inhibitor solution added at a concentration of 0.75 mM in order to saturate the Grb2 SH2 domain with the inhibitor. The buffer system consisted of 20 mM phosphate buffer (pH 6.3), 150 mM NaCl, and 0.05% NaN_3.

NMR experiments were run on Varian Unity Inova 800 and 600 MHz spectrometers at 25°C, using a triple-resonance probe equipped with a pulsed-field Z-axis gradient coil. Chemical shift assignments and acquisition of NOEs of the Grb2 SH2 domain were accomplished using a series of 3D heteronuclear experiments, according to a standard spectral data recorded on the $^{13}C/^{15}N$-labeled Grb2 SH2 domain protein complexed with the inhibitor in a 90% H_2O/10% ^2H_2O solution.

To complete the chemical shift assignments of the inhibitor bound to the Grb2 SH2 domain, 2D NOESY, 2D DQF-COSY and 2D TOCSY spectra were recorded of the inhibitor complexed with the $^2H/^{15}N$-labeled Grb2 SH2 domain dissolved in a ^2H_2O solution, and 2D ^{15}N-filtered TOCSY and 2D ^{15}N-filtered NOESY (Ogura et al. 1996) spectra were measured in a 90% H_2O solution.

Intermolecular NOEs between the Grb2 SH2 domain and the inhibitor were obtained from a 3D ^{13}C-filtered NOESY (Ogura et al. 1996) experiment recorded on the $^{13}C/^{15}N$-labeled Grb2 SH2 domain complexed with the inhibitor dissolved in a 90% H_2O/10% ^2H_2O solution and a 3D ^{15}N-edited NOESY experiment was recorded on the $^2H/^{15}N$-labeled Grb2 SH2 domain complexed with the inhibitor dissolved in a 90% H_2O/10% ^2H_2O solution. NMR data were processed using NMRPipe (Delaglio et al. 1995) and analyzed using in house software, Olivia (http://fermi.pharm.hokudai.ac.jp/olivia/).

Structure calculations

Structures were calculated using the program Cyana version 2.0 (Guntert 2004). As the first step in the calculation, an initial protein structure without the inhibitor was minimized until the rmsd of the main chain atoms was reduced to <1.0 Å. After evaluating assignments of NOEs and eliminating violated restraints, the final structure calculation of the protein–ligand complex was accomplished. To calculate the molecular complex of proteins and small organic compounds using Cyana, a residue library of the small molecule was defined and appended into a standard cyana.lib file. First, a PDB-formatted structural model of the inhibitor was created using the Dundee PRODRG2 server (http://davapc1.bioch.dundee.ac.uk/programs/prodrg/). Next, the resulting PDB file was manually converted into a Residue Library-formatted file in Cyana. Several key intermolecular distance restraints, which were mainly adopted from ^{15}N-edited NOESY spectrum recorded on the $^2H/^{15}N$-labeled Grb2 SH2 domain complexed with the inhibitor, were loosely applied for the first structure calculation of the complex. After the preliminary structures of the molecular complex were determined, additional protein–ligand intermolecular distance restraints derived from 3D ^{13}C-filtered NOESY data and the ligand–ligand intramolecular distance restraints were derived from the 2D NOESY data were incorporated into the Cyana calculations as manually added restraints between 3 and 6 Å with a rough calibration based on the NOE crosspeak intensity.

Dihedral angle restraints (62 ϕ and 62 ψ angles) were obtained by analysis of N, C^α, C^β, and H^α chemical shifts using the program TALOS (Cornilescu et al. 1999). Thirty-five hydrogen-bonding restraints were incorporated in the standard manner based on the preliminary structures and typical SH2 domain folding topology. A total of seven iterations for structural calculations and distance restraint assignments were run with Cyana on a parallel processing computer system equipped with 10 CPUs. One hundred structures were calculated, and the 20 structures having the lowest energies were adopted. The quality of each structure was assessed using the program Procheck-NMR (Laskowski et al. 1996). A list of all restraints and structural statistics is presented in Table 1. Figures were prepared using the programs PyMOL (http://pymol.sourceforge.net/) and MOLMOL (Koradi et al. 1996).

Results and discussion

Molecular mass in solution

Because Grb2 SH2 and the macrocyclic inhibitor complex existed as an intertwisted dimer in the crystal state (Phan et al. 2005), we first investigated whether Grb2 SH2 and the macrocyclic inhibitor complex for NMR analysis could form a dimer or not in solution. Analytical size exclusion chromatography of purified Grb2 SH2 and the macrocyclic inhibitor complex indicated that the complex formed a single species with no evidence of aggregation (Fig. 1). Calibration with molecular weight standards showed that Grb2 SH2 and the macrocyclic inhibitor complex corresponded to a globular protein of ~9 kDa, roughly consistent with the molecular mass calculated by the amino acid sequence and chemical formula of the macrocyclic inhibitor (~12 kDa). Moreover, It should be noted that the line widths of the Grb2 SH2 NMR resonances bound to the macrocyclic inhibitor were sufficiently small relevant to those of the molecular weight of the complex, so that we excluded the possibility of the dimer formation in solution. These results suggested that the domain-swapped dimer observed in the crystal structure was not formed in solution.

NMR assignments of the Grb2 SH2 domain complexed with the inhibitor

The ^{1}H, ^{13}C, and ^{15}N chemical shifts of the Grb2 SH2 domain complexed with the inhibitor were assigned from an array of heteronuclear multidimensional NMR experiments. Backbone sequential assignments for the protein were obtained by a conventional strategy using a combination of four triple-resonance experiments, 3D HN(CO)CA, 3D HNCA, 3D CBCA(CO)NH, and 3D CBCANH. Assignments of side chain atoms were completed by 3D HBHA(CO)NH, 3D HN(CA)HA, 3D C(CO)NH, and 4D HCCH-TOCSY spectra (Olejniczak et al. 1992).

NMR assignment of the inhibitor complexed with the Grb2 SH2 domain

In order to determine the structure of a protein-inhibitor complex, it is essential to distinguish the NMR signals of each component. Generally, in the case of a molecular complex of a $^{13}C/^{15}N$ labeled protein and an unlabeled inhibitor, the following steps are required. First, the NMR signals of the labeled protein are assigned using a series of triple resonance spectra. Next, the assignments of the unlabeled inhibitor in the complex are accomplished using a suite of filtering experiments. Although several filtering pulse schemes have been proposed (Breeze 2000), all of these schemes are based on utilizing large one-bond heteronuclear J couplings. For systems containing a wide range of one-bond J coupling constants, the filtering process should be repeated using different durations to eliminate undesirable signals, although repetition of the pulse schemes decreases the intensity of desirable signals. Therefore, it is generally difficult to eliminate undesirable signals completely while retaining desirable signals with reasonable signal-to-noise ratios. To overcome this problem, we utilized perdeuterated proteins to identify signals derived from inhibitors bound to proteins which have been successfully applied to the NMR analysis of protein–protein and protein–peptide interactions (Walters et al. 1997, Schwarz-Linek et al. 2003). We prepared NMR samples of the $^{15}N/^{2}H$-labeled Grb2 SH2 domain complexed with the high-affinity inhibitor dissolved in $^{2}H_2O$ and 90% H_2O/10% $^{2}H_2O$. Perdeuteration of the Grb2 SH2 domain completely eliminated the signals derived from the protein in $^{2}H_2O$ solution, so that all the resonances were derived from the inhibitor complexed with the Grb2 SH2 domain, thus simplifying the assignment process of the inhibitor. Figure 2 showed a comparison of 2D NOESY spectra (in $^{2}H_2O$) of the inhibitor complexed with the ^{15}N-labeled SH2 protein (Fig. 2a) and $^{15}N/^{2}H$-labeled SH2 protein (Fig. 2b). Figure 2a showed many NOE cross peaks that included intramolecular NOE connectivities within the Grb2 SH2 domain and the inhibitor as well as intermolecular NOE connectivities. Therefore, it was difficult to assign the resonances of the inhibitor unambiguously using the NOESY

spectrum. In Fig. 2b, on the other hand, due to perdeuteration of the protein, intramolecular NOE cross peaks derived from the inhibitor alone could be observed but those related to the SH2 domain were completely eliminated. Figure 3 showed an example of intramolecular NOE assignments of the inhibitor bound to the Grb2 SH2 domain together with the chemical structure of the inhibitor. Thus, the assignments of the non-exchangeable protons of the inhibitor bound to the protein were accomplished uniquely using the conventional 2D DQF-COSY, TOCSY, and NOESY spectrum in $^{2}H_2O$ solution. Moreover, the amide proton assignments of the inhibitor were carried out using 2D ^{15}N-filtered TOCSY and NOESY spectra measured in a 90% H_2O/10% $^{2}H_2O$ solution (data not shown). Thus, using $^{15}N/^{2}H$-labeled protein, we completed the proton assignments of the inhibitor bound to the Grb2 SH2 domain unambiguously.

Identification of intermolecular NOE correlations between the inhibitor and the Grb2 SH2 domain

We measured the two data sets of 3D NOESY spectra to detect intermolecular distance correlations for the structure determination of the inhibitor-Grb2 SH2 domain complex. Figure 4a showed strip plots of ^{1}H-^{1}H planes extracted from the 3D ^{13}C-filtered NOESY (Ogura et al. 1996) spectrum of the inhibitor bound to the $^{13}C/^{15}N$-labeled Grb2 SH2 domain dissolved in a 90% H_2O/10% $^{2}H_2O$ solution. In this spectrum, Pmp$^{\delta}$ and Pmp$^{\epsilon}$ protons of the inhibitor showed strong intermolecular NOE cross peaks with Ser96, His107, Phe108, and Lys109 of the Grb2 SH2 domain. These NOE correlations showed that the Pmp moiety of the inhibitor was bound to the pTyr-binding site of the protein. There were many intermolecular NOE signals between the inhibitor and the residues of the βD-strand of the protein. The main and side chain protons of Phe108 showed strong NOE correlations with the Pmp and Asn (pTyr+2) residue of the inhibitor. Lys109 showed a large number of NOE correlations with Pmp, the naphthylpropylamide group (NPA) (pTyr+3), and the three-carbon chain moiety (3CC). Moreover, Leu111 and Trp121 showed multiple NOE correlations with NPA (pTyr+3) and Asn (pTyr+2), respectively.

In order to detect the intermolecular NOE correlations between the amide protons of the protein and the inhibitor, we utilized a 3D ^{15}N-edited NOESY spectrum measured using a sample of the inhibitor complexed with the $^{15}N/^{2}H$-labeled Grb2 SH2 domain dissolved in a 90% H_2O/10% $^{2}H_2O$ solution. Due to the replacement of the non-exchangeable protons with deuterons, NOE cross peaks in the 3D NOESY spectrum were only derived from correlations between solvent-exchangeable (i.e., amide) protons of the Grb2 SH2 domain and the inhibitor protons. Therefore, the assignments of the intermolecular NOEs were significantly simplified. Figure 4b showed a comparison of cross-sections in the 3D ^{15}N-edited NOESY spectrum corresponding to the amide protons of His107, Phe108, and Lys109 recorded using the inhibitor complexed with the ^{15}N-labeled (left strips) and $^{15}N/^{2}H$-labeled (right strips) Grb2 SH2 domain in a 90% H_2O solution. While the NOESY strips recorded using the ^{15}N-labeled protein showed many cross peaks derived from the intra-molecular NOE correlations within the protein, use of the $^{15}N/^{2}H$-labeled Grb2 SH2 could eliminate intramolecular cross peaks within the protein and give intermolecular NOE cross peaks between the Grb2 SH2 domain and the inhibitor. Moreover, because the proton density of the Grb2 SH2 was reduced by deuteration, a number of long range intermolecular NOE correlations were detected. Thus, protein deuteration greatly simplified the assignment process of the intermolecular NOEs and facilitates unambiguous assignments of the inhibitor.

It should be mentioned here that perdeuterated proteins were useful especially for the assignments of protein-bound inhibitors such as medium-sized synthetic organic compounds and natural products, which could not be labeled with stable isotopes.

Structural description of the Grb2 SH2 domain complexed with the inhibitor

An overlay of the structures of the Grb2 SH2 domain and the inhibitor complex was shown in Fig. 5a. The atomic rmsd about the mean coordinates including the protein residues from Phe61 to Asp150 and the inhibitor, was 0.51 ± 0.07Å for the backbone atoms and 0.90 ± 0.08Å for all heavy atoms, where the backbone of the inhibitor was regarded as the macrocyclic frame. The Grb2 SH2 domain and the inhibitor have well defined structure.

The topology of the Grb2 SH2 domain was very similar to those of other SH2 domains. Figure 5b showed a ribbon diagram of the NMR-derived minimized mean structure of the Grb2 SH2 domain complexed with the inhibitor. The structure consisted of a three-stranded antiparallel β-sheet, composed of strands βB, βC and βD, which were flanked by two α-helices, αA and αB. The central β-sheet was extended by two short parallel strands (βA and βG) located on the opposite side to the inhibitor-binding site. The protein also contained a second, smaller β-sheet-like structure composed of strands βD′, βE and βF. The elementary residues constituting the secondary structure were, from N-terminus to C-terminus, 61–62 (βA), 67–77 (αA), 82–87 (βB), 95–100 (βC), 105–110 (βD), 111–112 (βD′), 118–119 (βE), 124–125 (βF), 128–138 (αB), 149–150 (βG). These were the same as the previously reported solution structures of Grb2 SH2 domain in both peptide-bound and peptide-free states (Thornton et al. 1996).

Specific interactions between Grb2 SH2 domain and the inhibitor

Figure 5b also showed the residues (with labels) that had appreciable NOE interactions and, therefore, had close contact with the inhibitor. The pTyr-binding pocket of the Grb2 SH2 domain was formed by the positively charged residues Arg67 (αA2), Arg86 (βB5), His107 (βD4) and Lys109 (βD6). In addition, Ser96 (βC3) also participated in the pocket. The aromatic ring of the pTyr-mimetic residue (Pmp) lay close to the βC and βD strands and had many NOEs with residues in the pocket, Ser96 (βC3), His107 (βD4), Phe108 (βD5) and Lys109 (βD6). The guanidium groups of the arginine residues in the pTyr-binding site could not be assigned under the present solution conditions. Although direct NOEs between the guanidium groups and the Pmp group of the inhibitor could not be obtained, the Pmp was clearly located proximal to Arg86 (βB5) at the bottom of the pTyr-binding pocket. The aromatic side chain of the Pmp residue was bound to the pTyr-binding pocket formed by a cluster of positively charged side chains as shown in Fig. 5b.

The Ac_6c (pTyr+1) residue of the inhibitor had intermolecular NOEs with Gln106 (βD3), His107 (βD4) and Phe108 (βD5) (Fig. 6a). The binding of Ac_6c (pTyr+1) to the Grb2 SH2 domain was mainly due to van der Waals interactions and, thus, the hydrophobic residue was required at the pTyr+1 position for specific binding. As shown in Fig. 6a, the cyclohexane ring of the Ac_6c moiety was well situated in a groove, formed by the hydrophobic moiety of Gln106, His107, and Phe108.

The asparagine (pTyr+2) of the ligand peptide was known as an essential residue for specific binding to the Grb2 SH2 domain. The aliphatic protons of this residue had strong intermolecular NOE interactions with the side chain of Trp121 (EF1). The H^{δ} of the Asn also had an intermolecular NOE interaction with the amide proton of Lys109 (βD6). However, because of lack of assignment of Leu120, we could not detect intermolecular NOE interactions between the H^{δ} of the Asn (pTyr+2) and the H^{α} of Leu120, which were observed in the solution structure of a Grb2 SH2 domain complexed with a Shc-derived ligand peptide (Ogura et al. 1999). The NMR signals of the H^{δ} protons of the Asn (pTyr+2) residue were shifted markedly to lower field (8.80 and 8.15 ppm, respectively). This lower-field shift was due to electric field effects, suggesting that these protons form hydrogen bonds with the carbonyl groups of the Grb2 SH2 domain as shown in Fig. 6b. These

hydrogen bonds between Asn-residue of the ligand and Lys109 have been detected on the crystal structure of Grb2 SH2 and the ligand peptide complex (Rahuel et al. 1996).

The side chain of the naphthylpropylamide group (pTyr+3) had multiple NOE contacts with both Lys109 and Leu111 (Fig. 6c). This residue at pTyr+3 was not conserved or type-conserved in peptidic ligands, but hydrophobic residues were preferred for specific binding with the Grb2 SH2 domain. In the present structure, we confirmed that the naphthyl group had hydrophobic interactions with the side chain of Leu111. Actually, the $H^{\delta 1}$ and $H^{\delta 2}$ protons of Leu111 were high field shifted to −0.31 and −0.19 ppm, respectively, consistent with magnetic shielding effects by the naphthyl ring.

The three-carbon chain moiety (3CC) consisting of $3CC^{\alpha}$, $3CC^{\beta}$ and $3CC^{\gamma}$, which maintains the macrocyclic structure of the inhibitor, had many NOE interactions with Lys109 of the Grb2 SH2 domain. In Fig. 6c, 3CC was located in close proximity to the aliphatic side chain of Lys109. Thus, 3CC played an important role, not only in the formation of the macrocyclic structure, but also in hydrophobic interactions with the side chain of Lys109.

Comparison of the solution structure of the inhibitor-bound Grb2 SH2 domain with the crystal structure

Phan et al. (2005) reported the crystal structure of a Grb2 SH2 domain complexed with a closely related macrocyclic inhibitor as was used in the NMR study. Interestingly, in the crystal structure, two SH2 domains formed a domain-swapped dimer that arose from exchanges of the C-terminal helix (αB). Thus, αB became detached from the rest of the molecule and associated with the other subunit, placing the EF, βF and FB loops in an extended conformation that started from the hinge point at Trp121 on the EF loop. It should be noted that the inhibitor used in the X-ray study contained a malonyl group instead of phosphono moiety and additional αCH_2CO_2H at the Pmp residue (Fig. 3a). Since we determined the well-defined structure of the Grb2 SH2 domain complexed with the NMR inhibitor, we could present a comparison of the two structures. First, the complex in the crystal structure showed a domain-swapped dimer and secondly, the Grb2 SH2 domain interacted with the inhibitors at four isolated sites, two of which were located proximal to the hinge region and the other two were located in the canonical Grb2 SH2 binding site. Using size exclusion chromatography and NMR spectroscopy, we confirmed that the NMR complex did not form a dimer, suggesting that the domain-swapped dimer in the crystal state might result from crystallization effects. In order to confirm this, we applied the analytical size exclusion chromatography experiment using Grb2 SH2 complexed with the X-ray inhibitor, showing that the complex existed as a monomer (data not shown).

Figure 7a and b showed the superposition of the solution structure with subunit-A and subunit-B of the crystal structure, each subunit corresponding to the split half of the domain-swapped dimer at the hinge. The rmsd values of C^{α} atoms for both the SH2 domain (residues 67–138, except for the loop regions and the inhibitor) between the solution structure and subunits-A and B are 1.03 and 1.09Å, respectively. Despite the domain-swapped dimer formation in the crystal state, the solution structure and subunits A and B of the crystal structure displayed similar backbones for the Grb2 SH2 domain and the macrocyclic inhibitor that was bound to the canonical binding site of the pTyr residue. However, a detailed inspection of the solution and crystal structures showed appreciable differences.

Figure 7a showed a superposition of the solution structure (green) and subunit-A of the crystal structure (pink). The BC loop region of subunit-A formed a closed conformation, with the side chains of the Ser88 and Ser90 residues interacting with the malonyl moiety of

the inhibitor. On the other hand, the solution structure showed an open BC loop conformation. Such open and closed conformational transitions have been frequently reported in SH2–ligand complexes (Eck et al. 1994; Mikol et al. 1995). The BC loop regions of SH2 domains seemed to be flexible and make an adjustment for distance between the BC loop and the phosphonate moiety of the ligand. It is also to be noted that the location of the naphthyl ring was appreciably different between subunit-A and the solution structure. The side chain of Trp121 swinged out to the opposite side of the inhibitor-binding site in subunit-A. Trp121 of the Grb2 SH2 domain was reported to be a key residue that forced a linear peptidic ligand to form a turn conformation. Therefore, the binding mode of the inhibitor in subunit-A was thought to be an artifact induced by a formation of the domain-swapped dimer. On the other hand, subunit-B was closely related to the solution structure (pink in Fig. 7b), including the location of the inhibitor on the Grb2 SH2 domain, the BC loop conformation and the side chain orientation of Trp121.

Another difference of the inhibitor in the crystal study against the NMR study was presence of α-CH_2CO_2H moiety in the pTyr-mimicking portion. Replacement of -H to -CH_2CO_2H produced an acidic moiety in this region and the side chain of Arg67 of Grb2 SH2 formed an electrostatic interaction with the carboxyl group of the pTyr-mimicking portion in the crystal structure. This acidic-basic interaction might contribute to improve the binding affinity of the inhibitor for Grb2 SH2 domain.

Consideration of inhibitor design derived from the solution structure of Grb2 SH2-inhibitor complex

The solution structure of the Grb2 SH2 domain complexed with the macrocyclic ligand provided insights into potential modifications of the macrocyclic ligand in at least four areas. (1) The binding of the pTyr+1 Ac_6c residue in a hydrophobic groove formed by residues Gln106 (βD3), His107 (βD4) and Phe108 (βD5) suggests modification of the Ac_6c ring, perhaps by extension of the ring δ-position; (2) The interactions of the naphthylpropyl group with the hydrophobic side chains of Lys109 (βD6) and Leu111 (βD8) suggests replacement of the naphthylpropyl moiety with other lipophilic functionality; (3) The interactions of the ring-closing propenyl chain segment with side chain methylenes of Lys109 (βD6) suggests exploration of alternate ring-closing strategies; (4) The open conformation of the phosphonate-binding BC loop suggests examining phosphate mimetics other than the phosphonomethyl group.

Conclusion

We have shown that perdeuterated proteins were useful for obtaining unambiguous assignments of protein-bound organic compounds and natural products that could not be labeled with stable isotopes. We accomplished the unique assignments of the intermolecular NOEs using perdeuterated proteins. Thus, we determined the high-resolution NMR structure of the complex of Grb2 SH2 and the macrocyclic inhibitor. The presented solution structure should provide a basis for further development of Grb2 SH2 domain inhibitors.

Supplementary Material

Refer to Web version on PubMed Central for supplementary material.

Acknowledgments

This work was supported by Grant-in-Aid for Scientific Research and the National Projects on Protein Structure and Functional Analysis from the Ministry of Education, Science and Culture of Japan. This research was also supported in part by the International Research Program of the NIH, Center for Cancer Research, National Cancer Institute.

References

Breeze AL. Isotope-filtered NMR methods for the study of biomolecular structure and interactions. Prog NMR Spectrosc. 2000; 36:323–372.

Buday L, Downward J. Epidermal growth factor regulates p21ras through the formation of a complex of receptor, Grb2 adapter protein, and Sos nucleotide exchange factor. Cell. 1993; 73:611–620. [PubMed: 8490966]

Burke TR Jr. Development of Grb2 SH2 domain signaling antagonists: a potential new class of antiproliferative agents. Int J Pept Res Therapeutics. 2006; 12:33–48.

Cornilescu G, Delaglio F, Bax A. Protein backbone angle restraints from searching a database for chemical shift and sequence homology. J Biomol NMR. 1999; 13:289–302. [PubMed: 10212987]

Daly RJ, Binder MD, Sutherland RL. Overexpression of the Grb2 gene in human breast cancer cell lines. Oncogene. 1994; 9:2723–2727. [PubMed: 8058337]

Delaglio F, Grzesiek S, Vuister GW, Zhu G, Pfeifer J, Bax A. NMRPipe: a multidimensional spectral processing system based on UNIX pipes. J Biomol NMR. 1995; 6:277–293. [PubMed: 8520220]

Domchek SM, Auger KR, Chatterjee S, Burke TR Jr, Shoelson SE. Inhibition of SH2 domain/phosphoprotein association by a nonhydrolyzable phosphonopeptide. Biochemistry. 1992; 31:9865–9870. [PubMed: 1382595]

Eck MJ, Atwell SK, Shoelson SE, Harrison SC. Structure of the regulatory domains of the Src-family tyrosine kinase Lck. Nature. 1994; 368:764–769. [PubMed: 7512222]

Furet P, Gay B, Garcia-Echeverria C, Rahuel J, Fretz H, Schoepfer J, Caravatti G. Discovery of 3-aminobenzyloxycarbonyl as an N-terminal group conferring high affinity to the minimal phosphopeptide sequence recognized by the Grb2-SH2 domain. J Med Chem. 1997; 40:3551–3556. [PubMed: 9357522]

Furet P, Gay B, Caravatti G, Garcia-Echeverria C, Rahuel J, Schoepfer J, Fretz H. Structure-based design and synthesis of high affinity tripeptide ligands of the Grb2-SH2 domain. J Med Chem. 1998; 41:3442–3449. [PubMed: 9719597]

Furet P, Garcia-Echeverria C, Gay B, Schoepfer J, Zeller M, Rahuel J. Structure-based design, synthesis, and X-ray crystallography of a high-affinity antagonist of the Grb2-SH2 domain containing an asparagine mimetic. J Med Chem. 1999; 42:2358–2363. [PubMed: 10395476]

Gale NW, Kaplan D, Lowenstein EJ, Schlessinger J, Bar-Sagi D. Grb2 mediates the EGF-dependent activation of guanine nucleotide exchange on Ras. Nature. 1993; 363:88–92. [PubMed: 8386805]

Gao Y, Voigt J, Wu JX, Yang D, Burke TR Jr. Macrocyclization in the design of a conformationally constrained Grb2 SH2 domain inhibitor. Bioorg Med Chem Lett. 2001a; 11:1889–1892. [PubMed: 11459654]

Gao Y, Wei CQ, Burke TR Jr. Olefin metathesis in the design and synthesis of a globally constrained Grb2 SH2 domain inhibitor. Org Lett. 2001b; 3:1617–1620. [PubMed: 11405669]

Garcia-Echeverria C, Furet P, Gay B, Fretz H, Rahuel J, Schoepfer J, Caravatti G. Potent antagonists of the SH2 domain of Grb2: optimization of the X_{+1} position of 3-amino-Z-Tyr (PO_3H_2)-X_{+1}-Asn-NH_2. J Med Chem. 1998; 41:1741–1744. [PubMed: 9599224]

Guntert P. Automated NMR structure calculation with CYANA. Methods Mol Biol. 2004; 278:353–378. [PubMed: 15318003]

Koradi R, Billeter M, Wuthrich K. MOLMOL: a program for display and analysis of macromolecular structures. J Mol Graph. 1996; 14:51–55. [PubMed: 8744573]

Kuriyan J, Cowburn D. Modular peptide recognition domains in eukaryotic signaling. Annu Rev Biophys Biomol Struct. 1997; 26:259–288. [PubMed: 9241420]

Laskowski RA, Rullmannn JA, MacArthur MW, Kaptein R, Thornton JM. AQUA and PROCHECK-NMR: programs for checking the quality of protein structures solved by NMR. J Biomol NMR. 1996; 8:477–486. [PubMed: 9008363]

Li N, Batzer A, Daly R, Yajnik V, Skolnik E, Chadrin P, Bar-Sagi D, Margolis B, Schlessinger J. Guanine-nucleotide-releasing factor hSos1 binds to Grb2 and links receptor tyrosine kinases to Ras signalling. Nature. 1993; 363:85–88. [PubMed: 8479541]

Lowenstein EJ, Daly RJ, Batzer AG, Li W, Margolis B, Lammers R, Ullrich A, Skolnik EY, Bar-Sagi D, Schlessinger J. The SH2 and SH3 domain-containing protein GRB2 links receptor tyrosine kinases to ras signaling. Cell. 1992; 70:431–442. [PubMed: 1322798]

Marengere LE, Pawson T. Structure and function of SH2 domains. J Cell Sci Suppl. 1994; 18:97–104. [PubMed: 7883800]

Mikol V, Baumann G, Keller TH, Manning U, Zurini MG. The crystal structures of the SH2 domain of p56lck complexed with two phosphonopeptides suggest a gated peptide binding site. J Mol Biol. 1995; 246:344–355. [PubMed: 7532720]

Ogura K, Terasawa H, Inagaki F. An improved double-tuned and isotope-filtered pulse scheme based on a pulsed field gradient and a wide-band inversion shaped pulse. J Biomol NMR. 1996; 8:492–498. [PubMed: 20859780]

Ogura K, Tsuchiya S, Terasawa H, Yuzawa S, Hatanaka H, Mandiyan V, Schlessinger J, Inagaki F. Solution structure of the SH2 domain of Grb2 complexed with the Shc-derived phosphotyrosine-containing peptide. J Mol Biol. 1999; 289:439–445. [PubMed: 10356320]

Olejniczak ET, Xu RX, Fesik SW. A 4D HCCH-TOCSY experiment for assigning the side chain 1H and 13C resonances of proteins. J Biomol NMR. 1992; 2:655–659. [PubMed: 1283353]

Phan J, Shi ZD, Burke TR Jr, Waugh DS. Crystal structures of a high-affinity macrocyclic peptide mimetic in complex with the Grb2 SH2 domain. J Mol Biol. 2005; 353:104–115. [PubMed: 16165154]

Pronk GJ, de Vries-Smits AMM, Buday L, Downward J, Maassen JA, Medema RH, Bos JL. Involvement of Shc in insulin- and epidermal growth factor-induced activation of p21ras. Mol Cell Biol. 1994; 14:1575–1581. [PubMed: 8114695]

Rahuel J, Gay B, Erdmann D, Strauss A, Garcia-Echeverria C, Furet P, Caravatti G, Fretz H, Schoepfer J, Grutter MG. Structural basis for specificity of GRB2-SH2 revealed by a novel ligand binding mode. Nat Struct Biol. 1996; 3:586–589. [PubMed: 8673601]

Rozakis-Adcock M, McGlade J, Mbamalu G, Pelicci G, Daly R, Li W, Batzer A, Thomas S, Brugge J, Pelicci PG, Schlessinger J, Pawson T. Association of the Shc and Grb2/Sem5 SH2-containing proteins is implicated in activation of the Ras pathway by tyrosine kinases. Nature. 1992; 360:689–692. [PubMed: 1465135]

Schlaepfer DD, Hanks SK, Hunter T, van der Geer P. Integrin-mediated signal transduction linked to Ras pathway by GRB2 binding to focal adhesion kinase. Nature. 1994; 372:786–791. [PubMed: 7997267]

Schwarz-Linek U, Werner JM, Pickford AR, Gurusiddappa S, Kim JH, Pilka ES, Briggs JA, Gough TS, Höök M, Campbell ID, Potts JR. Pathogenic bacteria attach to human fibronectin through a tandem beta-zipper. Nature. 2003; 423:177–181. [PubMed: 12736686]

Skolnik EY, Batzer A, Li N, Lee CH, Lowenstein LE, Mohammadi M, Margolis B, Schlessinger J. The function of GRB2 in linking the insulin receptor to Ras signaling pathways. Science. 1993a; 260:1953–1955. [PubMed: 8316835]

Skolnik EY, Lee CH, Batzer A, Vicentini LM, Zhou M, Daly R, Myers MJ Jr, Backer JM, Ullrich A, White MF, Schlessinger J. The SH2/SH3 domain-containing protein Grb2 interacts with tyrosine-phosphorylated IRS1 and Shc: implications for insulin control of ras signaling. EMBO J. 1993b; 12:1929–1936. [PubMed: 8491186]

Songyang Z, Shoelson SE, McGlade J, Olivier P, Pawson T, Bustelo XR, Barbacid M, Sabe H, Hanafusa H, Yi T, Ren R, Baltimore D, Ratnofsky S, Feldman RA, Cantley LC. Specific motifs recognized by the SH2 domains of Csk, 3BP2, fes/fps, Grb-2, SHPTP1, SHC, Syk and Vav. Mol Cell Biol. 1994; 14:2777–2785. [PubMed: 7511210]

Thornton KH, Mueller WT, McConnell P, Zhu G, Saltiel AR, Thanabal V. Nuclear magnetic resonance solution structure of the growth factor receptor-bound protein 2 Src homology 2 domain. Biochemistry. 1996; 35:11852–11864. [PubMed: 8794768]

Tsuchiya S, Ogura K, Hatanaka H, Nagata K, Terasawa H, Mandiyan V, Schlessinger J, Aimoto S, Ohta H, Inagaki F. Solution structure of SH2 domain of Grb2/Ash complexed with EGF receptor derived phosphotyrosine containing peptide. J Biochem. 1999; 125:1145–1153.

Walters KJ, Matsuo H, Wagner G. A simple method to distinguish intermonomer nuclear overhauser effects in homodimeric proteins with C_2 symmetry. J Am Chem Soc. 1997; 119:5958–5959.

Yip SS, Crew AJ, Gee JM, Hui R, Blamey RW, Robertson JF, Nicholson RI, Sutherland RL, Daly RJ. Up-regulation of the protein tyrosine phosphatase SHP-1 in human breast cancer and correlation with GRB2 expression. Int J Cancer. 2000; 88:363–368. [PubMed: 11054664]

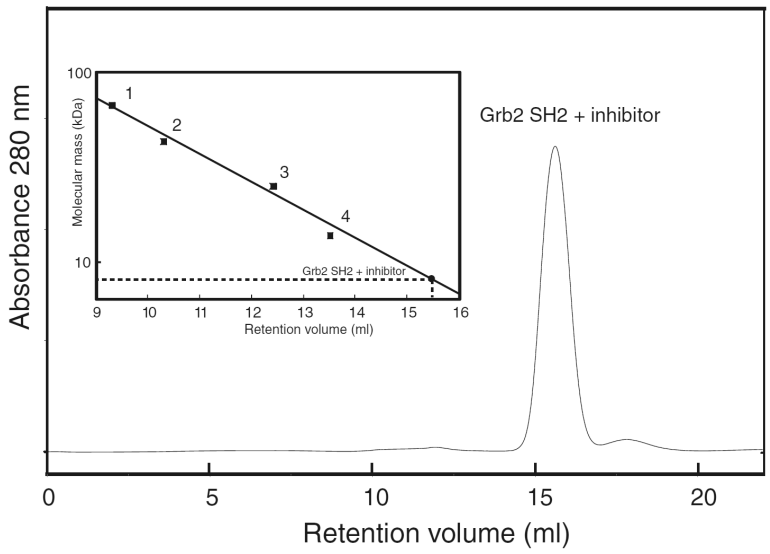

Fig. 1.

Analytical size exclusion chromatography profile for Grb2 SH2 and the macrocyclic inhibitor complex. The inset showed the calibration curve for molecular mass using standard proteins: bovine serum albumin (67 kDa, point 1), ovalbumin (43 kDa, point 2), chymotrypsinogen (25 kDa, point 3), and RNase A (13.7 kDa, point 4). Grb2 SH2 and the macrocyclic inhibitor complex eluted at a position corresponding to a molecular mass of ~9 kDa

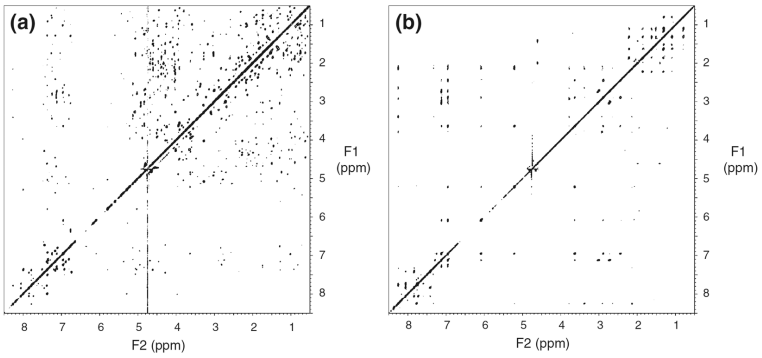

Fig. 2.

Selective observations of intramolecular NOE cross peaks within the inhibitor bound to Grb2 SH2. (**a**) 2D NOESY spectrum recorded using a complex of the inhibitor and ^{15}N-labeled Grb2 SH2 in a $^{2}H_2O$ solution, where intramolecular cross peaks derived from both the inhibitor and the protein and intermolecular cross peaks between the inhibitor and the protein were observed simultaneously. (**b**) 2D NOESY spectrum recorded using a complex of the inhibitor and ^{2}H/^{15}N-labeled Grb2 SH2 domain in a $^{2}H_2O$ solution. Cross peaks derived from the inhibitor were selectively observed

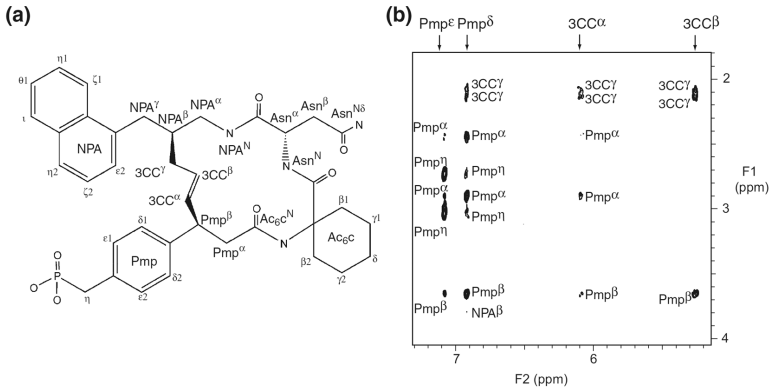

Fig. 3.

(**a**) Chemical structure of the inhibitor in which the protons were labeled. All proton signals were assigned by NMR. In the inhibitor used for the X-ray study, the phosphonomethyl group was replaced with a malonyl group and α-CH_2CO_2H was attached to the pTyr-mimicking portion. (**b**) Expanded view of 2D NOESY spectrum recorded using the complex of the inhibitor and $^{2}H/^{15}N$-labeled Grb2 SH2 domain in a $2H_2O$ solution. Inter- and intra-residue NOE connectivity of the inhibitor was labeled

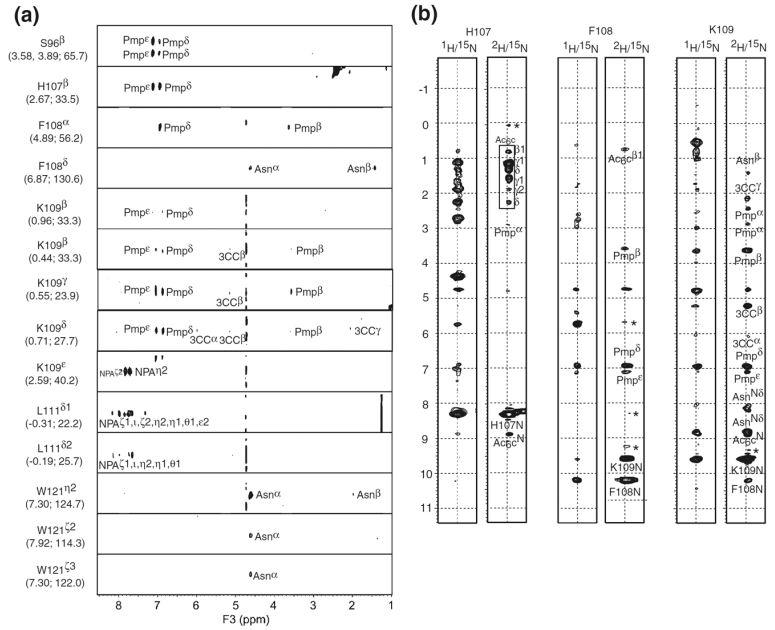

Fig. 4.

(**a**) Strip plots of ^{1}H-^{1}H planes extracted from a 3D ^{13}C-filtered NOESY spectrum recorded using the complex of the inhibitor and ^{13}C/^{15}N-labeled Grb2 SH2 domain in a 90% H_2O solution. Signals at 4.75 ppm on the F3-axis arised from the solvent. The resonance assignments and corresponding ^{1}H and ^{13}C chemical shifts of Grb2 SH2 domain were given in each strip. Intermolecular NOE correlations between the inhibitor and Grb2 SH2 domain were annotated. (**b**) Strip plots of ^{1}H-^{1}H planes extracted from 3D ^{15}N-edited NOESY recorded using a complex of the inhibitor and the ^{2}H/^{15}N-labeled Grb2 SH2 domain in a 90% H_2O solution. Intermolecular NOE correlations between amide protons of Grb2 SH2 and the inhibitor were labeled. Note that the intramolecular NOE correlations of amide-amide pairs of Grb2 SH2 domain were also observed. Signals at 4.75 ppm on the F1-axis arised from the solvent. Asterisk showed the artifact noise

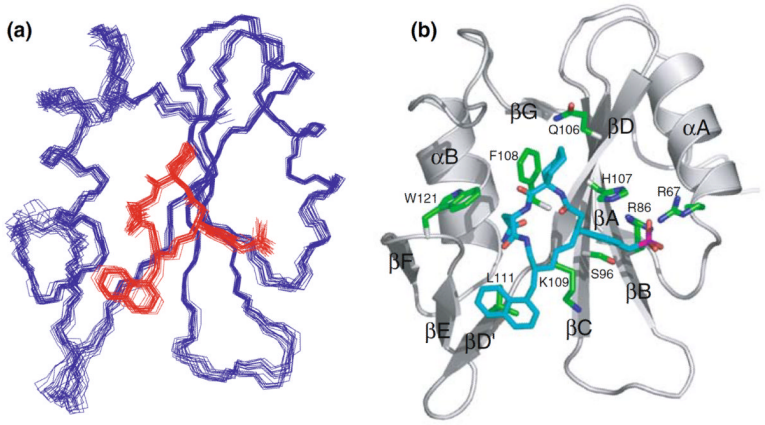

Fig. 5.

(**a**) Superposition of the 20 lowest energy structures of the Grb2 SH2 domain complexed with the inhibitor. Residues 60–152 of the Grb2 SH2 domain and the inhibitor were colored blue and red, respectively. Structures were superimposed by least square fit to average N, C^{α}, and C' coordinates of residues 60–152 of the Grb2 SH2 domain. (**b**) Ribbon model of the minimized and averaged structure of Grb2 SH2 domain complexed with the inhibitor (blue), where the side chains of protein residues involved in the binding interactions were shown in green. The regular secondary structural elements of Grb2 SH2 domain were labeled

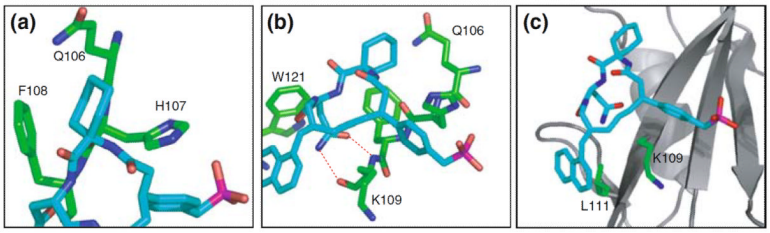

Fig. 6.

Details of the interaction between the inhibitor and the binding site of Grb2 SH2 domain. (**a**) pTyr+1 site; (**b**) pTyr+2 site; (**c**) pTyr+3 site. The inhibitors were shown as a stick model (cyan). Gln106, His107, Phe108, Lys109, Leu111 and Trp121 of Grb2 SH2 domain were shown as a stick model (green). Broken red lines in (**b**) indicated hydrogen bonds between the H^{δ} of Asn (pTyr+2) and Grb2 SH2 domain, as shown in the X-ray structure reported by Rahuel et al. (1996)

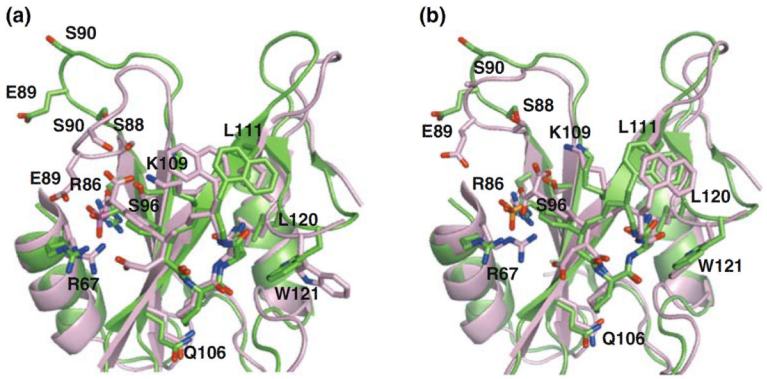

Fig. 7.

Superposition of the three dimensional structures of Grb2 SH2 domain with the inhibitor solved by NMR (green) and X-ray (pink, PDB ID 2AOB). Subunit-A and subunit-B of the crystal structures were shown in panel (**a**) and (**b**), respectively. Residues involving in recognition of the inhibitor were shown in stick models

Table 1

NMR-derived restraints and structural statistics

NOE upper distance restraints	
Short-range ($\|i-j\|<2$)	834
Medium-range ($2 \le \|i-j\| \le 4$)	217
Long-range ($\|i-j\|>4$)	518
Total	1569
Dihedral angle restraints (ψ and ϕ)	124
Hydrogen bonds restraints	35
Distance restraints	
Protein–ligand	84
Ligand–ligand	96
CYANA target function value ($Å^2$)	0.14
Number of violations	
Distance violations (>0.30 Å)	0
Dihedral angle violations (5.0°)	0
RMSD deviation from the averaged coordinates (Å)[a]	
Backbone atoms	0.51
Heavy atoms	0.90
Ramachandran analysis[b]	
Residues in most favored regions	76.1%
Residues in additional allowed regions	23.9%
Residues in generously allowed regions	0.0%
Residues in disallowed regions	0.0%

[a] For residues 61–150

[b] For residues 60–159